Activated microglia decrease histone acetylation and Nrf2-inducible anti-oxidant defence in astrocytes: Restoring effects of inhibitors of HDACs, p38 MAPK and GSK3β

Fernando Correa[a,*], **Carina Mallard**[b], **Michael Nilsson**[c], and **Mats Sandberg**[a]

[a]Department of Medical Biochemistry and Cell Biology, Institute of Biomedicine, University of Gothenburg, Sweden

[b]Department of Physiology, Institute of Neuroscience and Physiology, University of Gothenburg, Sweden

[c]CBR, Institute of Neuroscience and Physiology, University of Gothenburg, Sweden

Abstract

Histone deacetylase (HDAC) inhibitors have promising neuroprotective and anti-inflammatory properties although the exact mechanisms are unclear. We have earlier showed that factors from lipopolysaccharide (LPS)-activated microglia can down-regulate the astroglial nuclear factor-erythroid 2-related factor 2 (Nrf2)-inducible anti-oxidant defence. Here we have evaluated whether histone modification and activation of GSK3β are involved in these negative effects of microglia. Microglia were cultured for 24 h in serum-free culture medium to achieve microglia-conditioned medium from non-activated cells (MCM_0) or activated with 10 ng/mL of LPS to produce MCM_{10}. Astrocyte-rich cultures treated with MCM_{10} showed a time-dependent (0–72 h) increase in astroglial HDAC activity that correlated with lower levels of acetylation of histones H3 and H4 and decreased levels of the transcription factor Nrf2 and γ-glutamyl cysteine ligase modulatory subunit (γGCL-M) protein levels. The HDAC inhibitors valproic acid (VPA) and trichostatin-A (TSA) elevated the histone acetylation levels, restored the Nrf2-inducible anti-oxidant defence and conferred protection from oxidative stress-induced (H_2O_2) death in astrocyte-rich cultures exposed to MCM_{10}. Inhibitors of GSK3β (lithium) and p38 MAPK (SB203580) signaling pathways restored the depressed histone acetylation and Nrf2-related transcription whereas an inhibitor of Akt (Ly294002) caused a further decrease in Nrf2-related transcription. In conclusion, the study shows that well tolerated drugs such as VPA and lithium can restore an inflammatory induced depression in the Nrf2-inducible antioxidant defence, possibly via normalised histone acetylation levels.

Keywords

Neuroinflammation; Nrf2; Valproic acid; Trichostatin-A; Epigenetics

Introduction

Acetylation of lysine residues in histones and other proteins such as transcription factors constitutes one important mean of regulation of transcription and gene expression (Chuang

*Corresponding author at: Department of Medical Biochemistry and Cell Biology, Institute of Biomedicine, University of Gothenburg, PO BOX 420, 405 30 Göteborg, Sweden. Fax: +46 31 786 3840. Fernando.correa@medkem.gu.se (F. Correa).

et al., 2009). Histones acetyltransferases (HATs) and histones deacetylases (HDACs) constitute a group of enzymes that regulate acetylation/deacetylation. Inhibitors of HDACs are neuroprotective in several models of neurodegeneration (Chuang et al., 2009; Nalivaeva et al., 2009). For example, trichostatin-A (TSA) protected neurons in an *in vitro* and *in vivo* model of oxidative stress induced by depletion of glutathione (GSH) (Ryu et al. 2003). Likewise, astrocytes were less damaged by oxygen-glucose deprivation after TSA treatment via a reduced inflammatory reaction (Niu et al., 2009). Another HDAC inhibitor, valproic acid (VPA) has been shown to protect neurons in culture from glutamate-induced excitotoxicity (Bown et al., 2003). In a related study, it was shown that the effects of VPA were potentiated by simultaneous treatment with the glycogen synthase kinase-3 beta (GSK3β) inhibitor lithium (Leng et al., 2008; Adler et al., 2010). In models of stroke, a decreased acetylation could be normalised with HDAC inhibitors which also resulted in a lower infarct volume in parallel with reduced inflammation (Kim et al., 2007). Likewise, it has been shown that HDAC inhibitors reduce lippopolysaccharide (LPS)-induced release of pro-inflammatory cytokines in glial cells by a mechanism related to a reduced nuclear factor kappa-light-chain-enhancer of activated B cells (NFκB)-induced transcription (Faraco et al., 2009).

Activation of microglia, *i.e.* neuroinflammation, is an important mechanism in brain defence but over-activation can cause and/or propagate neuronal damage in neurodegenerative diseases and ageing (Block and Hong, 2007). The mechanisms behind the neurotoxicity relate to overproduction of neurotoxic pro-inflammatory cytokines as well as reactive oxygen and nitrogen species. Astroglial cells support and protect neurons in various ways, including the ability to elevate neuronal GSH (Dringen et al., 1999). One way to elevate GSH is via the redox sensitive transcription factor Nrf2 which is activated by oxidants and/ or electrophilic stress (Kobayashi et al., 2006). Once activated, Nrf2 can translocate into the nucleus and interact with specific DNA-sequences, called antioxidant responsive element (ARE, also named electrophile responsive element (EpRE)) (Kobayashi and Yamamoto, 2005). ARE-sites are located in promoter regions of genes encoding phase II antioxidant proteins such as the catalytic and modulatory subunits of γ-glutamyl cysteine ligase (γGCL-C and γGCL-M respectively) (Solis et al., 2002). Nrf2-*knock out* animals are over-sensitive to oxidative stress, their microglial cells are hyper-inflammatory and the animals develop white matter damage spontaneously (Innamorato et al., 2008; Hubbs et al., 2007). Overexpression of Nrf2 in astroglia protects against neuronal death in stroke and other disease models (Vargas et al., 2008). In addition it has been shown that brains from Alzheimer patients have low levels of Nrf2 in hippocampal astrocytes (Ramsey et al., 2007). Earlier studies have showed that GSK3β can down-regulate Nrf2 transcription in cultured neurons and in the hippocampus *in vivo* via export of Nrf2 from the nucleus and that this effect was blocked by inhibition of GSK3β via activation of phosphoinositol-3-kinase (PI3K) and Akt (Rojo et al., 2008a,b). We are interested in the effects of activated microglia on the antioxidant support of astrocytes. Recently we have shown that microglia activated for 24 h with LPS could up- or down-regulate the Nrf2 mediated antioxidant defence in astrocyte-rich cultures (Correa et al., 2011). The negative effects of LPS-activated microglial conditioned media on Nrf2 were associated with the activation of p38 MAPK (Correa et al., 2011). Here we address the possibility that the down-regulation of astroglial Nrf2-mediated transcription by microglia-conditioned media (MCMs) also involves epigenetic mechanisms such as methylation and acetylation of histones. Histone acetylation and/or methylation patterns in astrocyte-rich cultures exposed for 24 or 72 h to MCMs, the involvement of activated p38 MAPK and GSK3β, as well as the effects of the HDAC inhibitors VPA and TSA on the astroglial Nrf2-inducible antioxidant system and on the oxidative-induced cell death of astrocytes was evaluated.

Materials and methods

Reagents

Escherichia coli LPS (serotype O55:B5), valproic acid (VPA), trichostatin-A (TSA), lithium chloride (LiCl) and hydrogen peroxide (H_2O_2) were from Sigma (Stockholm, Sweden). SB203580 was from Cell Signaling Technology (Beverly, USA). Anti-acetyl-Histone H3, anti-acetyl-Histone H4 and anti-trimethyl-Lys9-Histone H3 were from Millipore (Solna, Sweden). Anti-phospho-p38 and anti-phospho-Ser9-GSK3β were from New England Biolabs (Beverly, USA). Anti-Nrf2 was from R&D Diagnostics (Minneapolis, USA). Anti-α-tubulin and anti-γGCL-M antibodies were from Santa Cruz Biotechnology (Heidelberg, Germany). Peroxidase-conjugated anti-rabbit and anti-mouse secondary antibodies were from Vector Laboratories (Burlingame, USA). Dubelcco's modified Eagle medium, poly-D-lysine; foetal bovine serum and penicillin/streptomycin solution were from Gibco/Invitrogen (Merelbeke, Belgium). Other common reagents were purchased from standard suppliers.

Primary microglia cultures and preparation of microglia-conditioned medium (MCM)

Primary mixed glial cultures were prepared as described previously (Correa et al., 2009). Briefly, after decapitation, forebrains of newborn Sprague–Dawley rats were dissociated mechanically, filtered through a 150 μm nylon mesh, resuspended in Dulbecco's modified Eagle's medium (DMEM) containing 10% heat-inactivated foetal bovine serum (FBS) and 1% penicillin/streptomycin and plated on poly-ᴅ-lysine-coated (PLD; 15 μg/ml) 75 cm^2 flasks (Falcon; Le Pont de Claix, France). After 15 days in culture the flasks were shaken at 230 rpm at 37 °C for 3 h to remove loosely adherent microglia. The supernatant was plated on 12-well culture plates for 2 h (5×10^4 cells/mL). After this, medium was changed to remove non-adherent cells. Cells were grown in a humidified environment containing 5% CO_2 and held at a constant temperature of 37 °C.

One hour prior to LPS exposure, medium was removed from microglial cultures and replaced by fresh serum-free DMEM. Then, stimulation with 10 ng/mL of LPS was performed for 24 h to achieve MCM_{10}. In parallel, cells were cultured for 24 h in medium without the addition of LPS to obtain non-activated microglia-conditioned medium, MCM_0. After collection, the conditioned media were sterile filtered through a 0.2 μm filter and frozen at −20 °C. Conditioned media derived from separate culture preparations were pooled before used.

Astrocyte-rich primary cultures and treatments

Cortical astrocyte-rich primary cultures were prepared from cortex of newborn (P1–P2) Sprague–Dawley rats as previously described (Hansson, 1984; Nodin et al., 2005). In brief, the rats were decapitated and cortices were carefully dissected. The tissue was mechanically passed through a nylon mesh (80 μm mesh size) into culture medium consisting of DMEM supplemented with 10% FBS and 1% penicillin/streptomycin. The cells were grown in 12 or 24 well plates at 37 °C in a humidified atmosphere of 5% CO_2. Cells were used after 7–10 days in culture when near confluency was reached.

For treatments, culture medium was replaced with fresh serum-free DMEM (control condition for 24 h) or exposed to undiluted MCMs for 24 h. For the 72 h experiments, cultures were exposed to MCMs for 48 h after which media was replaced with fresh MCM for 24 h. Control conditions for 72 h experiments were maintained with DMEM 1% FBS for 48 h after which media was replaced with fresh serum-free DMEM.

Histone deacetylase activity assay

Histone Deacetylase (HDAC) activity assay was performed using the commercial kit Fluor-de-Lys™ HDAC Fluorimetric Activity Assay Kit (Enzo Life Sciences; Exeter, UK) and following the manufacture's recommendations. The fluorescence intensity was measured in a fluorometer Spectra Max Gemini (Molecular Devices; Sunnyvale, USA) with an excitation wavelength of 350 nm and an emission wavelength of 500 nm.

Western blot analysis

After treatments, cultures were washed with ice-cold PBS and lysed in Tris-buffered saline pH 7.6 (TBS), containing 10% glycerol, 1% Nonidet P-40, EDTA 1 mM, EGTA 1 mM plus complete protease inhibitor cocktail (Roche; Stockholm, Sweden). Cell lysates were mixed with 5X Laemmeli sample buffer and boiled for 5 min. Then equal amount of protein (30 μg) was resolved on 10% SDS-PAGE in a MOPS or MES buffer (Invitrogen; Carlsbad, USA) and electroblotted at 40 V for 70 min at 4 °C to nitrocellulose (Bio-Rad; Hercules, USA). The membranes were blocked for 1 h at room temperature (RT) in 5% (w/v) dry skimmed milk (Semper Mjölk; Sundyberg, Sweden) in TBS with 0.1% Tween 20 (TBST). Then, the membranes were incubated overnight at 4 °C with the corresponding primary antibodies in 5% bovine serum albumin (BSA)-TBST, extensively washed with TBST solution and incubated with the correspondent secondary antibodies for 1 h at RT. Finally, the blots were rinsed and the peroxidase reaction was developed by enhanced chemiluminescence SuperSignal® West Dura Extended Duration Substrate (Thermo Scientific; Rockford, USA). Blots were stripped in RestoreTM Plus Western Blot Stripping Buffer (Thermo Scientific; Rockford, USA) and were reprobed sequentially.

Images were captured with a Fujifilm Image Reader LAS-1000 Pro v2.6 (Stockholm, Sweden) and the different band intensities (density arbitrary units) corresponding to immunoblot detection of protein samples were quantified using the Fujifilm Multi Gauge v3.0 software (Stockholm, Sweden).

Cytotoxicity and viability assay

Cell death was quantified by measurement of lactate dehydrogenase (LDH) release into the medium. LDH levels were determined using a commercial kit (Roche; Stockholm, Sweden). The LDH level corresponding to complete cell death was determined in sister cultures exposed to Triton X-100 (1% final concentration) for 24 h. In the case of 72 h exposure to different undiluted MCM, the media were changed to fresh undiluted MCM after 48 h of incubation and then further incubated for 24 h to complete the 72 h *in vitro*. Background LDH levels were determined in untreated sister cultures and subtracted from experimental values to yield the signal specific for experimentally-induced injury. Percentage of cell death in experimental conditions was calculated using the formula: [% of cell death = ((experimental value − BK) / (FK − BK)) 100], where BK stands for "blank" (sham wash) and FK stands for "full kill" (complete cell death).

Transfections and reporter gene analysis

The ARE reporter gene vector along with a *Renilla* luciferase expression vector from the Cignal™ Antioxidant Response Reporter Kit (SABiosciences; Frederick, USA) were transiently transfected into 10^5 astroglial cells using Lipofectamine™ Reagent (Invitrogen; Merelbeke, Belgium) according to the manufacturer's recommendation. After 24 h, medium was removed and changed with fresh serum-free DMEM and 2 h later, cells were stimulated as described in each case. Stimulation was allowed to proceed for another 24 h before cells were harvested, washed with phosphate saline buffer pH 7.4 (PBS) and lysed in cell lysis buffer (Promega; Nacka, Sweden). Luciferase activity (both firefly and *Renilla* luciferase

activity) was evaluated using the Dual-Luciferase® Reporter Assay System (Promega). Values were normalised to the *Renilla* luciferase activity (Promega). The Dual-Luciferase® Reporter Assay System refers to the simultaneous expression and measurement of two individual reporter enzymes within a single system. Thus, the "experimental" reporter (firefly luciferase) is correlated with the effect of specific experimental conditions whereas the activity of the cotransfected "control" (*Renilla* luciferase) reporter provides an internal control. Firefly and *Renilla* luciferase activity were measured as light emission over a period of 10 s each time in a VICTOR[2] Multilabel Counter (Wallac; Turku, Finland).

Statistical analysis

Results are presented as means ± standard error mean (SEM) of at least three separate experiments with different cell preparations. One-way ANOVA followed by the Bonferroni's post-hoc test for multiple comparison were used to determine statistical significance (95%; $p < 0.05$). If Levene's test for homogeneity of variances was significant then the Kruskal–Wallis nonparametric test was used.

Results

Effects of MCM on the astroglial HDAC activity and acetylation/methylation pattern of histones H3 and H4

To understand the role of HDACs in glial response to inflammatory conditions, we analysed the activity of histone deacetylases in astrocyte-rich cultures exposed for 24–72 h to control conditions, conditioned medium from unstimulated microglia (MCM_0) and conditioned medium from 10 ng/mL LPS-stimulated microglia (MCM_{10}) by means of a fluorometric kit. Fig. 1A shows the effects of MCMs on HDAC activity. Exposure to MCM_{10} induced an increased HDAC activity in astrocyte-rich cultures at 72 h, whereas MCM_0 and control conditions had no effects. Noteworthy, at 24 h MCM_{10} HDAC activity showed a tendency to higher levels when compared to MCM_0 or control conditions, albeit without statistical significance. Next we analysed the acetylation and methylation pattern of histones H3 and H4 in astrocyte-rich cultures after 24 and 72 h exposure to MCM_{10}. After 24 h there was a decrease in the acetylation pattern of histone H3 with a concomitant increase in the methylation pattern whereas no changes were observed in histone H4 (Fig. 1B, C). A prolonged (72 h) exposure to MCM_{10} resulted in a deacetylation of both histones H3 and H4 together with an increase methylation of histone H3(Fig. 1D, E). These observations demonstrates that deacetylation of histones H3 and H4 increase over time upon exposure to inflammatory conditions which correlate well with the MCM_{10}-induced increased HDAC activity.

Effect of HDAC inhibitors on the Nrf2-inducible antioxidant system

We have previously shown that exposure of astrocyte-rich cultures to MCM_{10} for 24 h reduced the astroglial GSH content and the expression of Nrf2 and γGCL-M (Correa et al., 2011). In an attempt to asses if the observed changes in acetylation levels (Fig. 1) could be involved in the down-regulation of Nrf2 and γGCL-M protein we treated cells with VPA (1 mM). Treatment with VPA (1 mM) produced a marked increase in the acetylation of histones H3 and H4 in parallel with a reversal of the negative effects of MCM_{10} on Nrf2 and γGCL–M protein levels (Fig. 2A–D).

Similar effects were observed for the other HDAC inhibitor used, TSA (10 nM). Thus, treatment with TSA (10 nM) for 24 h resulted in increased acetylation levels of histones H3 and H4 (Fig. 2E). Next, we exposed astrocyte–rich cultures to MCM_{10} for 24 h in the presence or absence of TSA (10 nM). As shown in Fig. 2G, treatment with TSA reversed the

effects of MCM_{10} on Nrf2 and γGCL-M levels. Densitometric analyses are shown in Fig. 2H.

Since both VPA and TSA were able to counteract the negative effects of MCM_{10} on Nrf2 and γGCL-M protein levels, we evaluated if exposure to HDAC inhibitors resulted in an increased resistance to oxidative stress. When astrocyte-rich cultures were exposed for 24 h to MCM_{10} and subsequently challenged with 250 μM H_2O_2 for three hours, cells were protected by the treatment with either 1 mM VPA (Fig. 3A) or 10 nM TSA (Fig. 3B).

Inhibition of p38 MAPK and GSK3β signalling pathways counteract the negative effects of MCM_{10} on the acetylation status of histone H3

Activation of p38 MAPK signalling pathway down-regulates the Nrf2-inducible antioxidant system (Naidu et al., 2009). We have previously shown that inhibition of p38 MAPK signalling with SB203580 (20 μM) inhibited the decrease in Nrf2 and γGCL-M protein levels and reduced H_2O_2 induced death in astrocyte-rich cultures exposed for 24 h to MCM_{10} (Correa et al., 2011). Since also the treatment with HDAC inhibitors restored the levels of Nrf2 and γGCL-M protein levels, we evaluated whether the activation of p38 MAPK could be involved in the acetylation status of histones. Astrocyte-rich cultures were exposed for 24 h to MCM_{10} in the presence or absence of SB203580 (20 μM) and the acetylation levels of histones H3 and H4 were assessed by western blot. As shown in Fig. 4A, inhibition of p38 MAPK resulted in normalisation of the acetylation levels of histone H3, suggesting that this signalling pathway is involved in the modulation of HDAC activities. Densitometric analyses are shown in Fig. 4B.

Inflammation also activates GSK3β signalling pathway which has been implicated in the regulation of the Nrf2-inducible antioxidant system (Rojo et al., 2008b; Rada et al., 2011). We performed a similar experiment as previously described, but this time we used lithium chloride (LiCl, 5 mM) as inhibitor of GSK3β. As shown in Fig. 4C, the inhibition of GSK3β restored the acetylation levels of histone H3, suggesting that this signalling pathway is also involved in the modulation of HDAC activities. Densitometric analyses are shown in Fig. 4D.

Next, and to confirm previous reports suggesting the participation of p38 MAPK and GSK3β in the modulation of Nrf2-mediated expression of antioxidant enzymes (Song et al., 2005; Cui et al., 2007; Rojo et al., 2008b; Naidu et al., 2009; Correa et al., 2011), we transiently transfected astrocyte-rich cultures with a commercial ARE-LUC reporter gene vector along with a *Renilla* luciferase expression vector. Transiently transfected cells were treated for 24 h with MCM_{10} in the presence or absence of the Akt inhibitor Ly294002 (10 μM). Exposure to MCM_{10} reduced activation of the ARE-promoter, reflected in the lower luciferase activity when compared to control. Inhibition of the Akt signalling pathway resulted in an even lower transcriptional activity of the ARE-promoter (Fig. 5A). When the transiently transfected astrocyte-rich cultures were exposed to MCM_{10} in the presence or absence of the GSK3β inhibitor LiCl (5 mM), the levels of luciferase activity detected were several times higher than in the MCM_{10} alone condition, suggesting that GSK3β is negatively involved in the modulation of the transcriptional activity of Nrf2 (Fig. 5B). Next, we exposed transiently transfected cells to MCM_{10} in the presence or absence of the p38 MAPK inhibitor SB203580 (20 μM). In this case, inhibition of p38 MAPK resulted in a higher luciferase activity when compared to the MCM_{10} alone condition, suggesting that this signalling pathway is negatively involved in the modulation of Nrf2 transcriptional activity (Fig. 5C). In order to investigate whether p38 MAPK and GSK3β signalling pathways could be involved in the modulation of Nrf2 transcriptional activity in an additive or potentiating fashion, we used both inhibitors SB203580 (20 μM) and LiCl (5 mM) together and analysed the luciferase activity. As shown in Fig. 5D, when both signalling

pathways were inhibited, the levels of luciferase activity were greater than those with the single inhibition of p38 MAPK or GSK3β. Therefore, the inhibition of p38 MAPK and GSK3β seems to have an additive effect on the Nrf2-mediated transcriptional activity.

Effect of prolonged HDAC inhibition on the Nrf2-inducible antioxidant system

HDAC activity remained elevated after 72 h of exposure to MCM_{10} showing an increased deacetylation of both histones H3 and H4 (Fig. 1A and D). In this condition, MCM_{10} also showed a decreased expression of Nrf2 and γGCL-M (Correa et al., 2011). We therefore evaluated long-term treatment with VPA (1 mM) and TSA (10 nM) on the acetylation pattern of histones H3 and H4 as well as the levels of Nrf2 and γGCL-M. As shown in Fig. 6A–B, treatment for 72 h with VPA 1 mM resulted in an increased acetylation of both histones, with more pronounced effects for H3 compared to H4. Treatment with VPA (1 mM) was able to reverse the effects of MCM_{10} on Nrf2 and γGCL-M levels (Fig. 6C, D).

Exposure to TSA (10 nM) for 72 h in control conditions resulted in increased acetylation levels of histones H3 and H4. Again, the levels of acetylation of histone H3 were higher than those of histone H4 (Fig. 6E). Next, we exposed astrocyte-rich cultures to MCM_{10} for 72 h in the presence or absence of TSA. As shown in Fig. 6GE–H, treatment with TSA at 10 nM reversed the negative effects of MCM_{10} on Nrf2 and γGCL-M levels.

Since both VPA and TSA were able to reverse the effects of MCM_{10} on Nrf2 and γGCL-M protein levels, we evaluated if exposure to HDAC inhibitors resulted in an increased resistance to oxidative stress. When astrocyte-rich cultures were exposed for 72 h to MCM_{10} and subsequently challenged with 250 μM H_2O_2 for 3 h, cells showed an elevated cytotoxicity but were protected by the treatment with either 1 mM VPA (Fig. 7A) or 10 nM TSA (Fig. 7B).

Discussion

Here we demonstrate that activated microglia can cause increased deacetylation of astroglial histone proteins and that HDAC inhibitors restore inflammation-induced down-regulation of antioxidant capacity in astrocytes and reduce cell death following oxidative stress.

The acetylation/methylation pattern of histones H3 and H4 in astrocyte-rich cultures was altered by the exposure to MCM_{10}. Pronounced effects on both down-regulation of acetylation and elevated methylation of histone H3 were observed. These types of modifications are in general associated with a decreased rate of gene transcription (Chuang et al., 2009) which may be an important factor involved in the down-regulation of Nrf2 in cultures exposed to MCM_{10}. These effects were pronounced by prolonging the treatment from 24 to 72 h and the acetylation levels were increased by the nonselective inhibitors of HDACs VPA and TSA. The pronounced effects of VPA and TSA on the acetylation levels could be related to a "double" effect via an inhibitory effect on HDACs and stimulatory effect on HAT p300 as shown recently for VPA-treated astrocytes (Marinova et al., 2011). Protein levels of Nrf2 and γGCL-M were down-regulated after both 24 and 72 h of treatment with MCM_{10} as reported earlier (Correa et al., 2011). Our observations demonstrating the negative effects of inflammation on Nrf2/γGCL-M levels are in agreement with the decreased levels of Nrf2 observed after treatment of a human monocyte/macrophage cell line with cigarette smoke condensate (Goven et al., 2009), lowered levels in chronic renal failure (Kim and Vaziri, 2010) and in hippocampal astrocytes in brains of humans suffering from Alzheimer's disease (Ramsey et al., 2007).

Several HDAC inhibitors have neuroprotective properties and have gained an increasing interest as potential drugs in neurodegenerative diseases (reviewed by Chuang et al., 2009).

The exact mechanisms behind the protective effects of HDAC inhibitors are not known but both normalisation of transcriptional dysfunction; decreased transcription and synthesis of various putative protective proteins have been shown. These include induction of heat shock protein 70 (HSP70) which inactivates NFκB in a model of cerebral ischemia (Zheng et al., 2008), increased expression by midbrain cells of glial cell-derived neurotrophic factor (GDNF) and brain-derived neurotrophic factor (BDNF) (Chen et al., 2006; Wu et al., 2008), anti-inflammatory effects by reducing microglia activation, TNFα release and nitric oxide production by LPS (Huuskonen et al., 2004; Chen et al., 2007) and direct effects on transcription factors or cofactors to transcription factors (Calao et al., 2008). It has also been shown that VPA induces apoptosis in murine microglial cells (Dragunow et al., 2006) by a p38 MAPK dependent mechanism (Xie et al., 2010) and microglial dysfunction, but not apoptosis, in human microglia (Gibbons et al., 2011). Here we add that HDAC inhibitors can restore inflammation-induced down-regulation of antioxidant capacity.

The synthesis of GSH is an important neuroprotective function of astrocytes which can be both up and down-regulated by inflammation *in vivo* and *in vitro* (Ballatori et al., 2009; Correa et al., 2011). The present study indicates that down-regulation of GSH in astrocytes, at least partly, could be due to epigenetic factors such as changes in the acetylation levels of histones. It remains to be determined how persistent this modulation is and whether, for example, the reported long-term effects of inflammation on the antioxidant parameters are due to such epigenetic effects (Yu et al., 2010). Other studies showing that epigenetic mechanisms regulate Nrf2 activation are that overexpression of HDAC2 in cell lines of airway epithelial cells decreased Nrf2 activation in parallel with elevated Nrf2 acetylation (Mercado et al., 2011). We have no explanation why acetylation in some case appears to decrease Nrf2 activation (Mercado et al., 2011) whereas in other cases (present work, Liu et al., 2008; Sun et al., 2009) the opposite is observed. It indicates that although acetylation appears to be important in the regulation of Nrf2 activation it is difficult to generalise the down-stream effects. In accordance with our results, it was shown in cells from Transgenic Adenocarcinoma of Mouse Prostate (TRAMP) mice that TSA in combination with a DNA methyltranferase inhibitor restored Nrf2 activation (Yu et al., 2010).

To get further insight into the mechanisms by which factors released from activated microglia activate HDACs and reduce the antioxidant defence system in astrocyte-rich cultures, we used inhibitors of pathways that we and others have earlier shown to be activated in inflammation (Branger et al., 2002; Hee et al., 2002; Bendotti et al., 2005; Beurel and Jope, 2008; Naidu et al., 2009; Correa et al., 2011). These experiments were performed using a plasmid containing ARE sequences coupled to a luciferase reporter gene. The luciferase activity is thus proportional to the ARE-mediated transcriptional activity of Nrf2. Treatment of astrocyte-rich cultures with MCM_{10} reduced ARE-mediated transcription as expected since Nrf2 protein expression was decreased. Likewise, the positive effect of lithium and SB203580 on the ARE-promoter activity is likely due to elevated or normalised levels of Nrf2 protein. The negative effect of GSK3β on Nrf2-mediated transcription was also corroborated by that Akt inhibition reduced ARE-mediated transcription, as Akt inactivates GSK3β. Our observations fit well with previous studies that identified GSK3β as an important kinase for the negative modulation of Nrf2-induced transcriptional activity (Rojo et al., 2008b; Rada et al., 2011). Co-treatment with p38 MAPK and GSK3β inhibitors resulted in an additive positive effect on ARE-mediated transcription, suggesting that Nrf2-mediated transcription may be regulated by both kinases in parallel. The mechanisms behind the down-regulation of Nrf2 protein and Nrf2-mediated transcription by activated GSK3β and p38 MAPK is not known. It has been suggested that GSK3β can phosphorylate Nrf2 followed by transport to the cytoplasm and degradation via the proteasome pathway (Salazar et al., 2006). A similar mechanism has been proposed for p38 MAPK actions on Nrf2 (Naidu et al., 2009). Another possibility is that p38 MAPK

phosphorylates the p65 subunit of NFκB, which then transport Keap1 to the nucleus (Yu et al., 2011). The increased nuclear level of Keap1 restricts Nrf2 binding to ARE-sequences and directs Nrf2 to proteasomal degradation (Yu et al., 2011).

Interestingly, the inhibition of p38 MAPK and GSK3β activation normalised both the down-regulation of acetylation of histone H3 as well as the decreased protein levels of Nrf2 and γGCL-M observed after exposure to MCM_{10}. The molecular mechanism behind the positive effects of GSK3β and p38 MAPK inhibition on the acetylation levels of histones remains to be clarified. Lithium has earlier been shown to enhance the effects of HDAC inhibitors but had no effect by itself on histone acetylation, suggesting that lithium is not a HDAC inhibitor *per se* (Leng et al., 2008; Adler et al., 2010). One possibility is that HDACs are direct targets of GSK3β and p38 MAPK activity. Indeed, it was recently demonstrated that GSK3β directly phosphorylates and activates HDAC3, which then exerts neurotoxic effects (Bardai and D'Mello, 2011).

VPA is a pleiotrophic molecule that can inhibit GSK3β (Kim et al., 2005) and can activate p38 MAPK (Xie et al., 2010). On the other hand, as TSA, which does not block GSK3β activation (Leng et al., 2008), resulted in similar positive effects on Nrf2, γGCL-M and acetylation of histone H3 as VPA, we favour that VPA and TSA exert their protective effects on the Nrf2-system mainly via inhibition of HDACs and not via direct effects on p38 MAPK/GSK3β.

The protective effects of increased acetylation/decreased methylation pattern of histones on the Nrf2-system by TSA and VPA could be a result of an increase in a protein that saves Nrf2 from degradation. One such protein is p21[waf1/cipl], which is elevated by TSA and rescues cortical neurons treated with TSA (Inokoshi et al., 1999). Interestingly, it was found that elevated levels of p21[waf1/cipl] were sufficient but not necessary for mediating the effects of HDAC inhibitors (Inokoshi et al., 1999). It should be noted that the activity of several transcription factors, including Nrf2, can be regulated by acetylation. In cell lines, Nrf2 is acetylated at the transcription site by the HAT p300/CBP followed by an increased expression of ARE-driven genes, including γGCL-M (Sun et al., 2009). Also HDACs can bind closely to the transcription machinery of Nrf2 and NF-kB/p65 was recently shown to deprive CBP from Nrf2 which facilitated binding of the co-repressor HDAC3 to Maf proteins, the binding partners of Nrf2 (Liu et al., 2008). This resulted in a local histone hypoacetylation (Liu et al., 2008) which *per se* may reduce the transcription of components in the Nrf2 system. The binding of either HAT or HDAC to the Nrf2 transcription machinery is thus highly important and can have effects on transcription both via direct acetylation of Nrf2 and/or changed acetylation levels of histones that are local to the ARE-binding sites (Sun et al., 2009; Liu et al., 2008).

Whatever the mechanisms behind the positive effects of HDAC inhibitors are, it is obvious that inhibition of HDACs leads to a plethora of neuroprotective effects. Here we add that well tolerated drugs such as VPA and lithium restore the Nrf2-inducible antioxidant defence in parallel with normalised acetylation levels of histones in astrocyte-rich cultures. This effect may, in part, underlie the neuroprotection and the inhibition of neuroinflammation exerted by HDAC inhibitors.

Acknowledgments

Abbreviations

γGCL	gamma-glutamylcysteine ligase
γGCL-C	gamma-glutamylcysteine ligase catalytic subunit
γGCL-M	gamma-glutamylcysteine ligase modulatory subunit
GSH	glutathione
GSK3β	glycogen synthase kinase-3 beta
HAT	histone acetyltransferase
HDAC	histone deacetylase
Keap1	Kelch-like ECH-associated protein 1
ERK1/2	extracellular regulated kinase
JNK	c-Jun N-terminal kinase
LPS	lipopolysaccaride
MAPKs	mitogen-activated protein kinases
MCM	microglia-conditioned medium
MEK	mitogen-activated protein kinase
NF-κB	nuclear factor kappa-light-chain-enhancer of activated B cells
Nrf2	nuclear factor-erythroid 2-related factor 2
*t*BHQ	tert-butylhydroquinone
TSA	trichostatin A
VPA	valproic acid

References

Adler JT, Hottinger DG, Kunnimalaiyaan M, Chen H. Inhibition of growth in medullary thyroid cancer cells with histone deacetylase inhibitors and lithium chloride. J. Surg. Res. 2010; 159:640–644. [PubMed: 19394967]

Ballatori N, Krance SM, Notenboom S, Shi S, Tieu K, Hammond CL. Glutathione dysregulation and the etiology and progression of human diseases. Biol. Chem. 2009; 390:191–214. [PubMed: 19166318]

Bardai FH, D'Mello SR. Selective toxicity by HDAC3 in neurons: regulation by Akt and GSK3{beta}. J. Neurosci. 2011; 31:1746–1751. [PubMed: 21289184]

Bendotti C, Bao CM, Cheroni C, Grignaschi G, Lo CD, Peviani M, Tortarolo M, Veglianese P, Zennaro E. Inter- and intracellular signaling in amyotrophic lateral sclerosis: role of p38 mitogen-activated protein kinase. Neurodegener. Dis. 2005; 2:128–134. [PubMed: 16909017]

Beurel E, Jope RS. Differential regulation of STAT family members by glycogen synthase kinase-3. J. Biol. Chem. 2008; 283:21934–21944. [PubMed: 18550525]

Block ML, Hong JS. Chronic microglial activation and progressive dopaminergic neurotoxicity. Biochem. Soc. Trans. 2007; 35:1127–1132. [PubMed: 17956294]

Bown CD, Wang JF, Young LT. Attenuation of *N*-methyl-d-aspartate-mediated cytoplasmic vacuolization in primary rat hippocampal neurons by mood stabilizers. Neuroscience. 2003; 117(4): 949–955. [PubMed: 12654346]

Branger J, van den Blink B, Weijer S, Madwedm J, Bos CL, Gupta A, Yong CL, Polmar SH, Olszyna DP, Hack CE, van Deventer SJ, Peppelenbosch MP, van der Poll T. Anti-inflammatory effects of a p38 mitogen-activated protein kinase inhibitor during human endotoxemia. J. Immunol. 2002; 168:4070–4077. [PubMed: 11937566]

Calao M, Burny A, Quivy V, Dekoninck A, Van Lint C. A pervasive role of histone acetyltransferases and deacetylases in an NF-kappaB-signaling code. Trends Biochem. Sci. 2008; 33(7):339–349. [PubMed: 18585916]

Chen PS, Peng GS, Li G, Yang S, Wu X, Wang CC, Wilson B, Lu RB, Gean PW, Chuang DM, Hong JS. Valproate protects dopaminergic neurons in midbrain neuron/glia cultures by stimulating the release of neurotrophic factors from astrocytes. Mol. Psychiatry. 2006; 11:1116–1125. [PubMed: 16969367]

Chen PS, Wang CC, Bortner CD, Peng GS, Wu X, Pang H, Lu RB, Gean PW, Chuang DM, Hong JS. Valproic acid and other histone deacetylase inhibitors induce microglial apoptosis and attenuate lipopolysaccharide-induced dopaminergic neurotoxicity. Neuroscience. 2007; 149:203–212. [PubMed: 17850978]

Chuang DM, Leng Y, Marinova Z, Kim HJ, Chiu CT. Multiple roles of HDAC inhibition in neurodegenerative conditions. Trends Neurosci. 2009; 32:591–601. [PubMed: 19775759]

Correa F, Docagne F, Mestre L, Clemente D, Hernangómez M, Loría F, Guaza C. A role for CB2 receptors in anandamide signalling pathways involved in the regulation of IL-12 and IL-23 in microglial cells. Biochem. Pharmacol. 2009; 77:86–100. [PubMed: 18848818]

Correa F, Ljundggren E, Mallard C, Nilsson M, Weber SG, Sandberg M. The Nrf2-inducible antioxidant defence in astrocytes can be both up- and down-regulated by activated microglia: involvement of p38 MAPK. Glia. 2011; 59(5):785–799. [PubMed: 21351160]

Cui J, Shao L, Young LT, Wang JF. Role of glutathione in neuroprotective effects of mood stabilizing drugs lithium and valproate. Neuroscience. 2007; 144:1447–1453. [PubMed: 17184924]

Dragunow M, Greenwood JM, Cameron RE, Narayan PJ, O'Carroll SJ, Pearson AG, Gibbons HM. Valproic acid induces caspase 3-mediated apoptosis in microglial cells. Neuroscience. 2006; 140(4):1149–1156. [PubMed: 16600518]

Dringen R, Pfeiffer B, Hamprecht B. Synthesis of the antioxidant glutathione in neurons: supply by astrocytes of CysGly as precursor for neuronal glutathione. J. Neurosci. 1999; 19:562–569. [PubMed: 9880576]

Faraco G, Pittelli M, Cavone L, Fossati S, Porcu M, Mascagni P, Fossati G, Moroni F, Chiarugi A. Histone deacetylase (HDAC) inhibitors reduce the glial inflammatory response in vitro and in vivo. Neurobiol. Dis. 2009; 36:269–279. [PubMed: 19635561]

Gibbons HM, Smith AM, Teoh HH, Bergin PM, Mee EW, Faull RL, Dragunow M. Valproic acid induces microglial dysfunction, not apoptosis, in human glial cultures. Neurobiol. Dis. 2011; 41(1):96–103. [PubMed: 20816784]

Goven D, Boutten A, Leçon-Malas V, Boczkowski J, Bonay M. Prolonged cigarette smoke exposure decreases heme oxygenase-1 and alters Nrf2 and Bach1 expression in human macrophages: roles of the MAP kinases ERK(1/2) and JNK. FEBS Lett. 2009; 583:3508–3518. [PubMed: 19822148]

Hansson E. Cellular composition of a cerebral hemisphere primary culture. Neurochem. Res. 1984; 9:153–172. [PubMed: 6204217]

Hee HB, Choi J, Holtzman DM. Evidence that p38 mitogen-activated protein kinase contributes to neonatal hypoxic–ischemic brain injury. Dev. Neurosci. 2002; 24:405–410. [PubMed: 12640179]

Hubbs AF, Benkovic SA, Miller DB, O'Callaghan JP, Battelli L, Schwegler-Berry D, Ma Q. Vacuolar leukoencephalopathy with widespread astrogliosis in mice lacking transcription factor Nrf2. Am. J. Pathol. 2007; 170(6):2068–2076. [PubMed: 17525273]

Huuskonen J, Suuronen T, Nuutinen T, Kyrylenko S, Salminen A. Regulation of microglial inflammatory response by sodium butyrate and short-chain fatty acids. Br. J. Pharmacol. 2004; 141:874–880. [PubMed: 14744800]

Innamorato NG, Rojo AI, García-Yagüe AJ, Yamamoto M, de Ceballos ML, Cuadrado A. The transcription factor Nrf2 is a therapeutic target against brain inflammation. J. Immunol. 2008; 181:680–689. [PubMed: 18566435]

Inokoshi J, Katagiri M, Arima S, Tanaka H, Hayashi M, Kim YB, Furumai R, Yoshida M, Horinouchi S, Omura S. Neuronal differentiation of neuro 2a cells by inhibitors of cell cycle progression, trichostatin A and butyrolactone I. Biochem. Biophys. Res. Commun. 1999; 256:372–376. [PubMed: 10079191]

Kim HJ, Vaziri ND. Contribution of impaired Nrf2-Keap1 pathway to oxidative stress and inflammation in chronic renal failure. Am. J. Physiol. Renal Physiol. 2010; 298:F662–F671. [PubMed: 20007347]

Kim AJ, Shi Y, Austin RC, Werstuck GH. Valproate protects cells from ER stress-induced lipid accumulation and apoptosis by inhibiting glycogen synthase kinase-3. J. Cell Sci. 2005; 118:89–99. [PubMed: 15585578]

Kim HJ, Rowe M, Ren M, Hong JS, Chen PS, Chuang DM. Histone deacetylase inhibitors exhibit anti-inflammatory and neuroprotective effects in a rat permanent ischemic model of stroke: multiple mechanisms of action. J. Pharmacol. Exp. Ther. 2007; 321:892–901. [PubMed: 17371805]

Kobayashi M, Yamamoto M. Molecular mechanisms activating the Nrf2-Keap1 pathway of antioxidant gene regulation. Antioxid. Redox Signal. 2005; 7:385–394. [PubMed: 15706085]

Kobayashi A, Kang MI, Watai Y, Tong KI, Shibata T, Uchida K, Yamamoto M. Oxidative and electrophilic stresses activate Nrf2 through inhibition of ubiquitination activity of Keap1. Mol. Cell. Biol. 2006; 26:221–229. [PubMed: 16354693]

Leng Y, Liang MH, Ren M, Marinova Z, Leeds P, Chuang DM. Synergistic neuroprotective effects of lithium and valproic acid or other histone deacetylase inhibitors in neurons: roles of glycogen synthase kinase-3 inhibition. J. Neurosci. 2008; 28:2576–2588. [PubMed: 18322101]

Liu GH, Qu J, Shen X. NF-kappaB/p65 antagonizes Nrf2-ARE pathway by depriving CBP from Nrf2 and facilitating recruitment of HDAC3 to MafK. Biochim. Biophys. Acta. 2008; 1783(5):713–727. [PubMed: 18241676]

Marinova Z, Leng Y, Leeds P, Chuang DM. Histone deacetylase inhibition alters histone methylation associated with heat shock protein 70 promoter modifications in astrocytes and neurons. Neuropharmacology. 2011; 60(7–8):1109–1115. [PubMed: 20888352]

Mercado N, Thimmulappa R, Thomas CM, Fenwick PS, Chana KK, Donnelly LE, Biswal S, Ito K, Barnes PJ. Decreased histone deacetylase 2 impairs Nrf2 activation by oxidative stress. Biochem. Biophys. Res. Commun. 2011; 406(2):292–298. [PubMed: 21320471]

Naidu S, Vijayan V, Santoso S, Kietzmann T, Immenschuh S. Inhibition and genetic deficiency of p38 MAPK up-regulates heme oxygenase-1 gene expression via Nrf2. J. Immunol. 2009; 182:7048–7057. [PubMed: 19454702]

Nalivaeva NN, Belyaev ND, Turner AJ. Sodium valproate: an old drug with new roles. Trends Pharmacol. Sci. 2009; 30:509–514. [PubMed: 19762089]

Niu F, Zhang X, Chang L, Wu J, Yu Y, Chen J, Xu Y. Trichostatin A enhances OGD-astrocyte viability by inhibiting inflammatory reaction mediated by NF-kappaB. Brain Res. Bull. 2009; 78:342–346. [PubMed: 19103266]

Nodin C, Nilsson M, Blomstrand F. Gap junction blockage limits intercellular spreading of astrocytic apoptosis induced by metabolic depression. J. Neurochem. 2005; 94:1111–1123. [PubMed: 16092948]

Rada P, Rojo AI, Chowdhry S, McMahon M, Hayes JD, Cuadrado A. SCF (beta-TrCP) promotes Glycogen synthase kinase-3-dependent degradation of the Nrf2 transcription factor in a Keap1-independent manner. Mol. Cell. Biol. 2011; 31(6):1121–1133. [PubMed: 21245377]

Ramsey CP, Glass CA, Montgomery MB, Lindl KA, Ritson GP, Chia LA, Hamilton RL, Chu CT, Jordan-Sciutto KL. Expression of Nrf2 in neurodegenerative diseases. J. Neuropathol. Exp. Neurol. 2007; 66:75–85. [PubMed: 17204939]

Rojo AI, Rada P, Egea J, Rosa AO, López MG, Cuadrado A. Functional interference between glycogen synthase kinase-3 beta and the transcription factor Nrf2 in protection against kainate-induced hippocampal cell death. Mol. Cell. Neurosci. 2008a; 39:125–132. [PubMed: 18619545]

Rojo AI, Sagarra MR, Cuadrado A. GSK-3beta down-regulates the transcription factor Nrf2 after oxidant damage: relevance to exposure of neuronal cells to oxidative stress. J. Neurochem. 2008b; 105(1):192–202. [PubMed: 18005231]

Ryu H, Lee J, Olofsson BA, Mwidau A, Dedeoglu A, Escudero M, Flemington E, Azizkhan-Clifford J, Ferrante RJ, Ratan RR. Histone deacetylase inhibitors prevent oxidative neuronal death independent of expanded polyglutamine repeats via an Sp1-dependent pathway. Proc. Natl. Acad. Sci. U. S. A. 2003; 100:4281–4286. [PubMed: 12640146]

Salazar M, Rojo AI, Velasco D, de Sagarra RM, Cuadrado A. Glycogen synthase kinase-3beta inhibits the xenobiotic and antioxidant cell response by direct phosphorylation and nuclear exclusion of the transcription factor Nrf2. J. Biol. Chem. 2006; 281:14841–14851. [PubMed: 16551619]

Solis WA, Dalton TP, Dieter MZ, Freshwater S, Harrer JM, He L, Shertzer HG, Nebert DW. Glutamate-cysteine ligase modifier subunit: mouse Gclm gene structure and regulation by agents that cause oxidative stress. Biochem. Pharmacol. 2002; 63:1739–1754. [PubMed: 12007577]

Song IS, Tatebe S, Dai W, Kuo MT. Delayed mechanism for induction of gamma-glutamylcysteine synthetase heavy subunit mRNA stability by oxidative stress involving p38 mitogen-activated protein kinase signaling. J. Biol. Chem. 2005; 280:28230–28240. [PubMed: 15946948]

Sun Z, Chin YE, Zhang DD. Acetylation of Nrf2 by p300/CBP augments promoter-specific DNA binding of Nrf2 during the antioxidant response. Mol. Cell. Biol. 2009; 29:2658–2672. [PubMed: 19273602]

Vargas MR, Johnson DA, Sirkis DW, Messing A, Johnson JA. Nrf2 activation in astrocytes protects against neurodegeneration in mouse models of familial amyotrophic lateral sclerosis. J. Neurosci. 2008; 28(50):13574–13581. [PubMed: 19074031]

Wu X, Chen PS, Dallas S, Wilson B, Block ML, Wang CC, Kinyamu H, Lu N, Gao X, Leng Y, Chuang DM, Zhang W, Lu RB, Hong JS. Histone deacetylase inhibitors up-regulate astrocyte GDNF and BDNF gene transcription and protect dopaminergic neurons. Int. J. Neuropsychopharmacol. 2008; 11:1123–1134. [PubMed: 18611290]

Xie N, Wang C, Lin Y, Li H, Chen L, Zhang T, Sun Y, Zhang Y, Yin D, Chi Z. The role of p38 MAPK in valproic acid induced microglia apoptosis. Neurosci. Lett. 2010; 482(1):51–56. [PubMed: 20621161]

Yu S, Khor TO, Cheung KL, Li W, Wu TY, Huang Y, Foster BA, Kan YW, Kong AN. Nrf2 expression is regulated by epigenetic mechanisms in prostate cancer of TRAMP mice. PLoS One. 2010; 5:e8579. [PubMed: 20062804]

Yu M, Li H, Liu Q, Liu F, Tang L, Li C, Yuan Y, Zhan Y, Xu W, Li W, Chen H, Ge C, Wang J, Yang X. Nuclear factor p65 interacts with Keap1 to repress the Nrf2-ARE pathway. Cell. Signal. 2011; 23(5):883–892. [PubMed: 21262351]

Zheng Z, Kim JY, Ma H, Lee JE, Yenari MA. Anti-inflammatory effects of the 70 kDa heat shock protein in experimental stroke. J. Cereb. Blood Flow Metab. 2008; 28:53–63. [PubMed: 17473852]
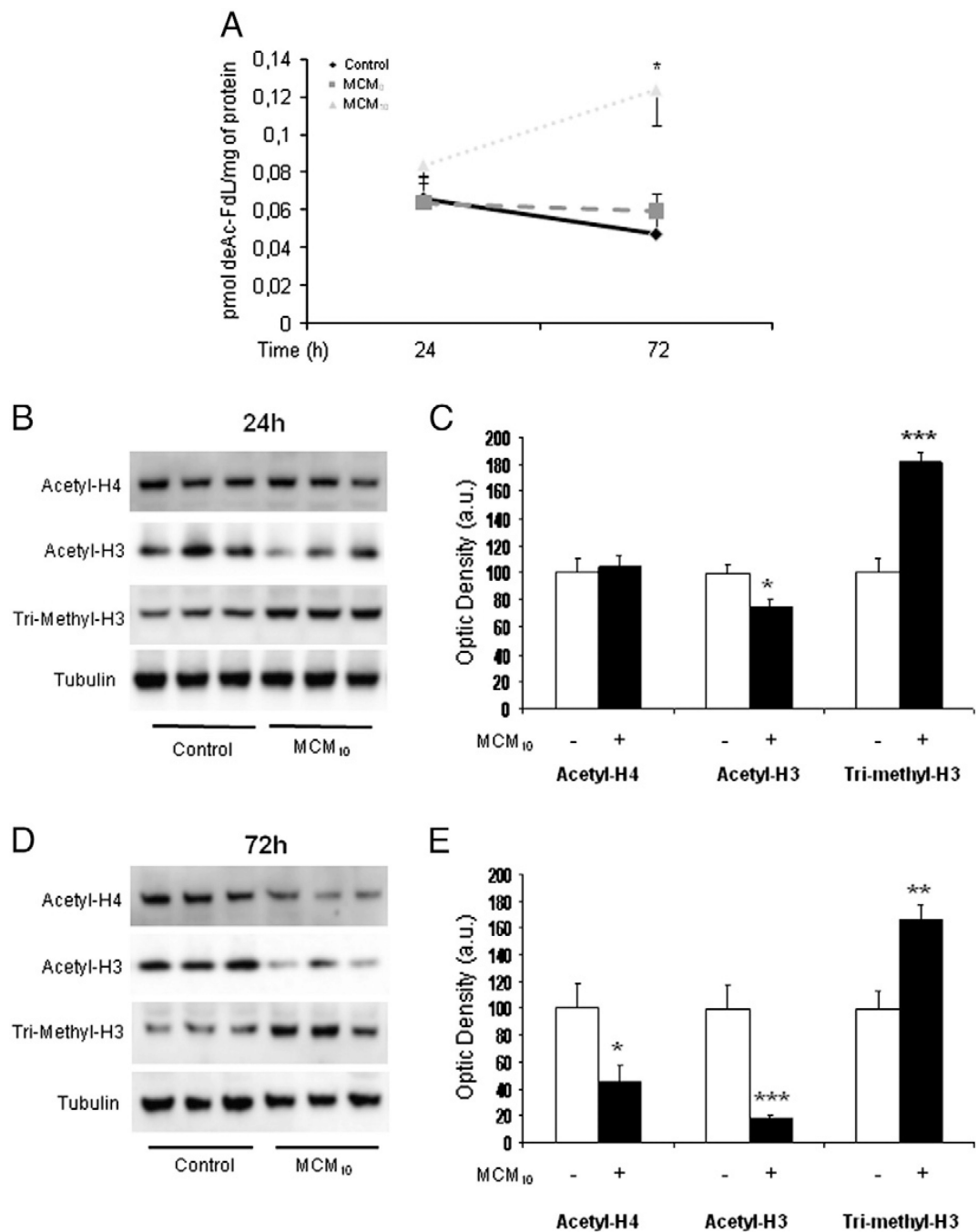
Fig. 1.
(A) Histone deacetylase (HDAC) activity in astrocyte-rich cultures exposed to control conditions (see Material and methods for details), conditioned-medium from unstimulated microglia (MCM_0) or conditioned-medium from 10 ng/mL LPS-stimulated microglia (MCM_{10}). HDAC activity started to increase already after 24 h and was elevated 72 h in cells treated with MCM_{10}. HDAC activity remained elevated at 72 h post-treatment whereas in the case of MCM_0 and control conditions there were no changes. Results are mean ± SEM. Statistics: *p<0.05 *vs* same time-point control. (B) Exposure of astrocyte-rich cultures to MCM_{10} for 24 h induced a decrease in the acetylation levels of histone H3 (acetyl-H3) with a concomitant increase in the methylation levels of this histone (tri-methyl-H3) when

compared to control conditions. No changes in the acetylation levels of histone H4 (acetyl-H4) were observed. A representative blot is shown. (C) Densitometric analysis of acetyl-H4, acetyl-H3 and tri-methyl-H3 protein expression in astrocyte-rich cultures exposed for 24 h to control conditions or MCM_{10}. Data are plotted as ratio of the protein of interest/tubulin obtained in each condition. Statistics: *p<0.05 *vs* control; ***p<0.005 *vs* control. (D) Exposure of astrocyte-rich cultures to MCM_{10} for 72 h induced a decrease in the acetylation levels of histone H3 (acetyl-H3) and histone H4 (acetyl-H4) followed by an increase in the methylation levels of this histone (tri-methyl-H3) when compared to control conditions. A representative blot is shown. (E) Densitometric analysis of acetyl-H4, acetyl-H3 and tri-methyl-H3 protein expression in astrocyte-rich cultures exposed for 72 h to control conditions or MCM_{10}. Data are plotted as ratio of the protein of interest/tubulin obtained in each condition. Statistics: *p<0.05 *vs* control; **p<0.01 *vs* control; ***p<0.005 *vs* control.
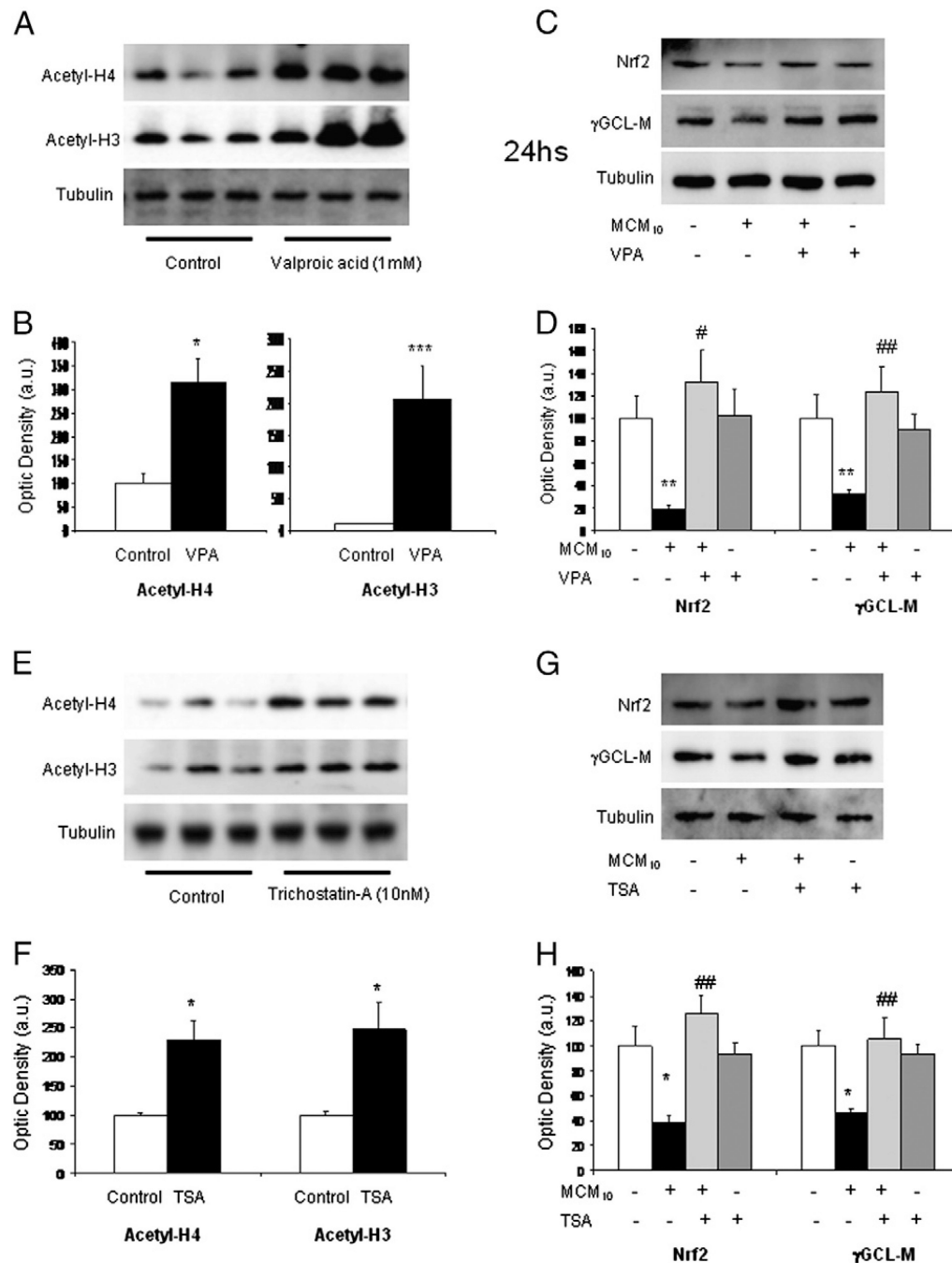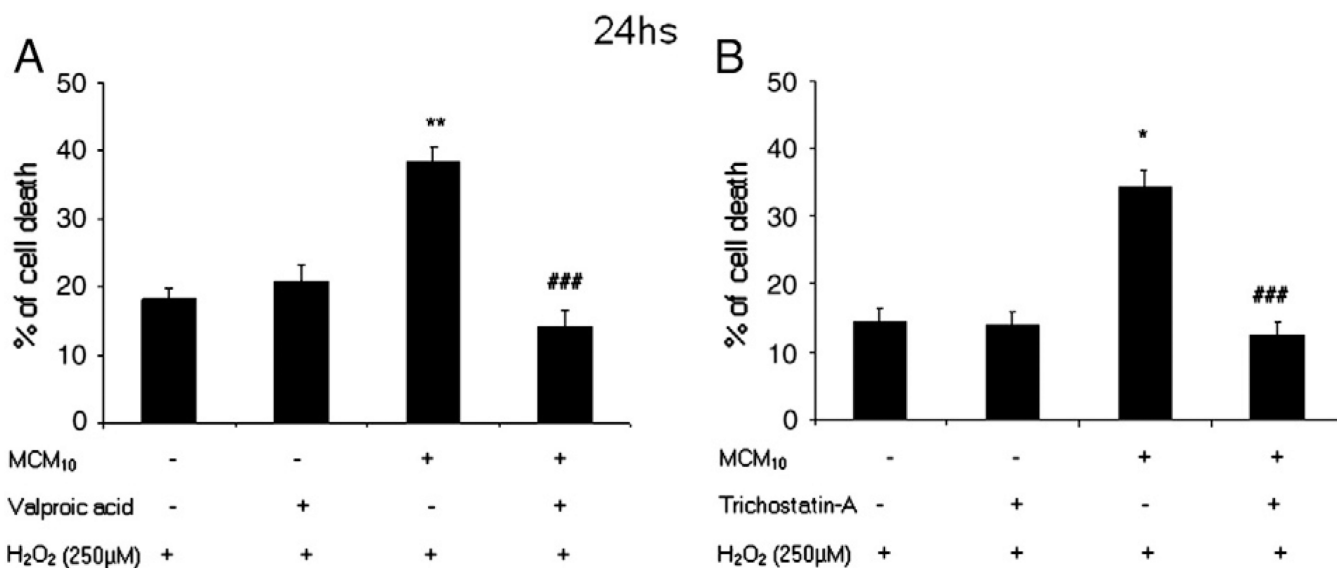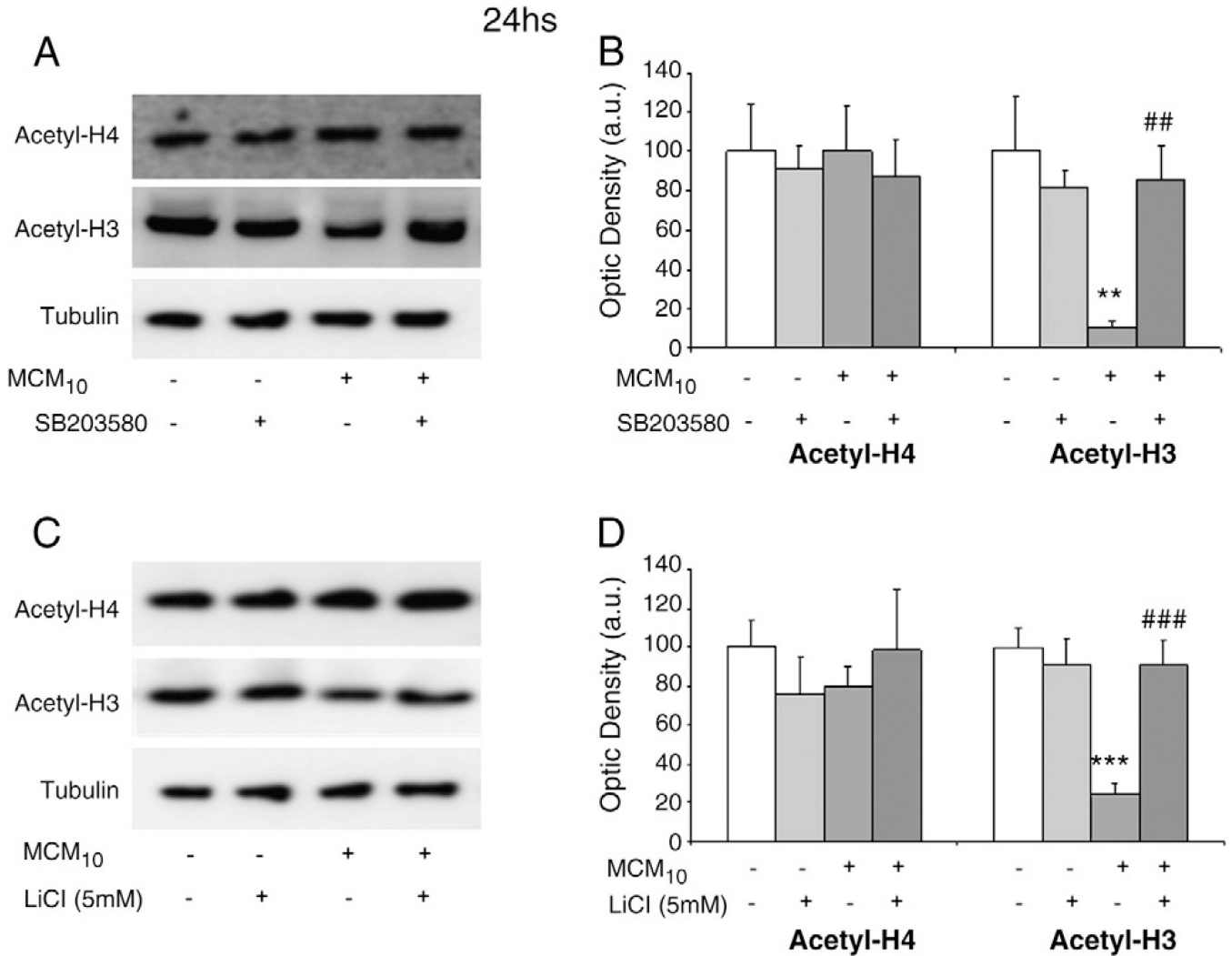
Fig. 2.
(A) Treatment with the HDAC inhibitor valproic acid (VPA; 1 mM) for 24 h induced an increase in the acetylation levels of histones H3 and H4 in astrocyte-rich cultures. A representative blot is shown. (B) Densitometric analysis of acetyl-H4 and acetyl-H3 protein expression in astrocyte-rich cultures exposed for 24 h to control conditions or VPA 1 mM. Data are plotted as ratio of the protein of interest/tubulin obtained in each condition. Statistics: *p<0.05 *vs* control; ***p<0.005 *vs* control. (C) Treatment with VPA (1 mM) for 24 h restored the levels of Nrf2 and γGCL-M that were down-regulated by the exposure to MCM_{10}. A representative blot is shown. (D) Densitometric analysis of Nrf2 and γGCL-M protein expression in astrocyte-rich cultures exposed for 24 h to control conditions or
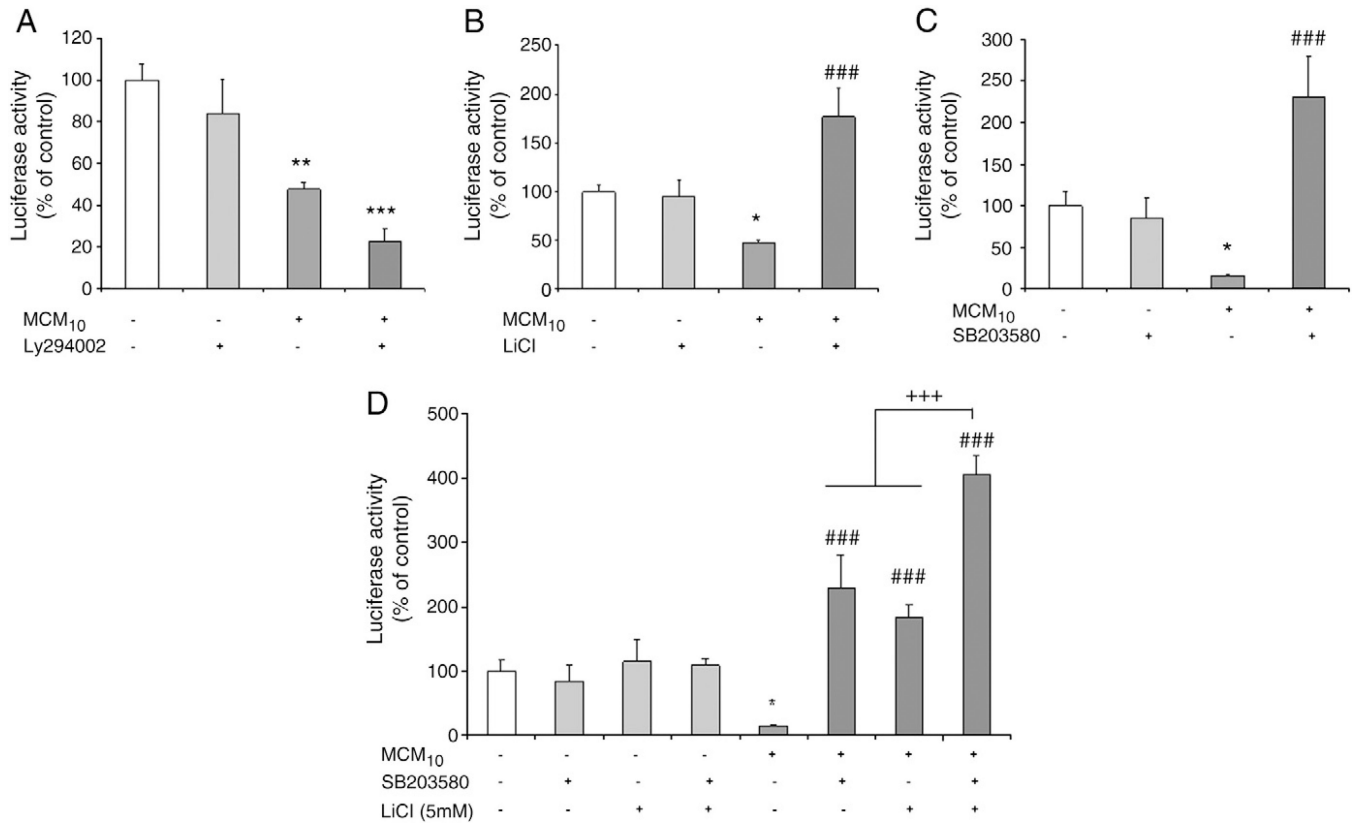
MCM_{10} in the presence or absence of VPA (1 mM). Data are plotted as ratio of the protein of interest/tubulin obtained in each condition. Statistics: **p<0.01 *vs* control; #p<0.05 *vs* MCM_{10}; ##p<0.01 *vs* MCM_{10}. (E) Treatment with the HDAC inhibitor trichostatin-A (TSA; 10 nM) for 24 h induced an increase in the acetylation levels of histone H3 and histone H4. A representative blot is shown. (F) Densitometric analysis of acetyl-H4 and acetyl-H3 protein expression in astrocyte-rich cultures exposed for 24 h to control conditions or TSA (10 nM). Data are plotted as ratio of the protein of interest/tubulin obtained in each condition. Statistics: *p<0.05 *vs* control. (G) Treatment with TSA (10 nM) for 24 h restored the levels of Nrf2 and γGCL-M that were down-regulated by the exposure to MCM_{10}. A representative blot is shown. (H) Densitometric analysis of Nrf2 and γGCL-M protein expression in astrocyte-rich cultures exposed for 24 h to control conditions or MCM_{10} in the presence or absence of TSA (10 nM). Data are plotted as ratio of the protein of interest/ tubulin obtained in each condition. Statistics: *p<0.05 *vs* control; ##p<0.01 *vs* MCM_{10}.

Fig. 3.
(A) Cells were exposed for 24 h to control conditions or MCM_{10} in the presence or absence of VPA (1 mM). Twenty-four hours later, cells were exposed to hydrogen peroxide (250 μM) for 3 h and cell death was assessed by measuring the LDH released into the medium. Exposure to MCM_{10} rendered astrocyte-rich cultures more susceptible to oxidative stress induced by hydrogen peroxide showing higher levels of cell loss. This effect was reversed by the treatment with VPA (1 mM). The results shown are the mean ± SEM. Statistics: **$p<0.01$ *vs* control; ###$p<0.005$ *vs* MCM_{10}. (B) Cells were exposed for 24 h to control conditions or MCM_{10} in the presence or absence of TSA (10 nM). Twenty-four hours later, cells were exposed to hydrogen peroxide (250 μM) for 3 h and cell death was assessed by measuring the LDH released into the bathing medium. Exposure to MCM_{10} rendered astrocyte-rich cultures more susceptible to oxidative stress induced by hydrogen peroxide showing higher levels of cell loss. This effect was reversed by the treatment with TSA 10 nM. The results shown are the mean ± SEM. Statistics: *$p<0.05$ *vs* control; ###$p<0.005$ *vs* MCM_{10}.

Fig. 4.
(A) Treatment with the p38 MAPK inhibitor SB203580 (20 μM) for 24 h reversed the negative effects of MCM_{10} on the acetylation levels of histone H3. No changes were observed in the acetylation levels of histone H4. A representative blot is shown. (B) Densitometric analysis of acetyl-H4 and acetyl-H3 protein expression in astrocyte-rich cultures exposed for 24 h to control conditions or MCM_{10} in the presence or absence of SB203580 (20 μM). Data are plotted as ratio of the protein of interest/tubulin obtained in each condition. Statistics: **$p<0.01$ *vs* control; ##$p<0.01$ *vs* MCM_{10}. (C) Treatment with the GSK3β inhibitor lithium chloride (LiCl; 5 mM) for 24 h reversed the effects of MCM_{10} on the acetylation levels of histone H3. No changes were observed in the acetylation levels of histone H4. A representative blot is shown. (B) Densitometric analysis of acetyl-H4 and acetyl-H3 protein expression in astrocyte-rich cultures exposed for 24 h to control conditions or MCM_{10} in the presence or absence of LiCl (5 mM). Data are plotted as ratio of the protein of interest/tubulin obtained in each condition. Statistics: ***$p<0.005$ *vs* control; ###$p<0.005$ *vs* MCM_{10}.

Fig. 5.
(A) Astrocyte-rich cultures were transiently transfected for 24 h with the ARE reporter gene vector along with a *Renilla* luciferase expression vector. Transiently transfected cells were treated for 24 h with MCM_{10} in the presence or absence of the Akt inhibitor Ly294002 (10 μM). MCM_{10} induced a reduced ARE-related transcription activity, expressed by a lower luciferase activity. This effect was enhanced when the Akt signalling pathway was inhibited. Statistics: **p<0.01 *vs* control; ***p<0.005 *vs* control. (B) Transiently transfected cells were treated for 24 h with MCM_{10} in the presence or absence of the GSK3β inhibitor LiCl (5 mM). Inhibition of GSK3β signalling pathway was able to fully reverse the effects of MCM_{10} on the ARE-related transcription activity. Statistics: *p<0.05 *vs* control; ###p<0.005 *vs* MCM_{10}. (C) Transiently transfected cells were treated for 24 h with MCM_{10} in the presence or absence of the p38 MAPK inhibitor SB203580 (20 μM). Inhibition of p38 MAPK signalling pathway fully reversed the effects of MCM_{10} on the ARE promoter activity. Statistics: *p<0.05 *vs* control; ###p<0.005 *vs* MCM_{10}. (D) Transiently transfected cells were treated for 24 h with MCM_{10} in the presence or absence of the GSK3β inhibitor LiCl (5 mM), the p38 MAPK inhibitor SB203580 (20 μM) or the two inhibitors combined. Inhibition of both GSK3β and p38 MAPK signalling pathways had additive effects and was able to fully reverse the effects of MCM_{10} on the ARE promoter activity. Statistics: *p<0.05 *vs* control; ###p<0.005 *vs* MCM_{10}; +++p<0.05 *vs* MCM_{10} + SB203580 or MCM_{10} + LiCl.
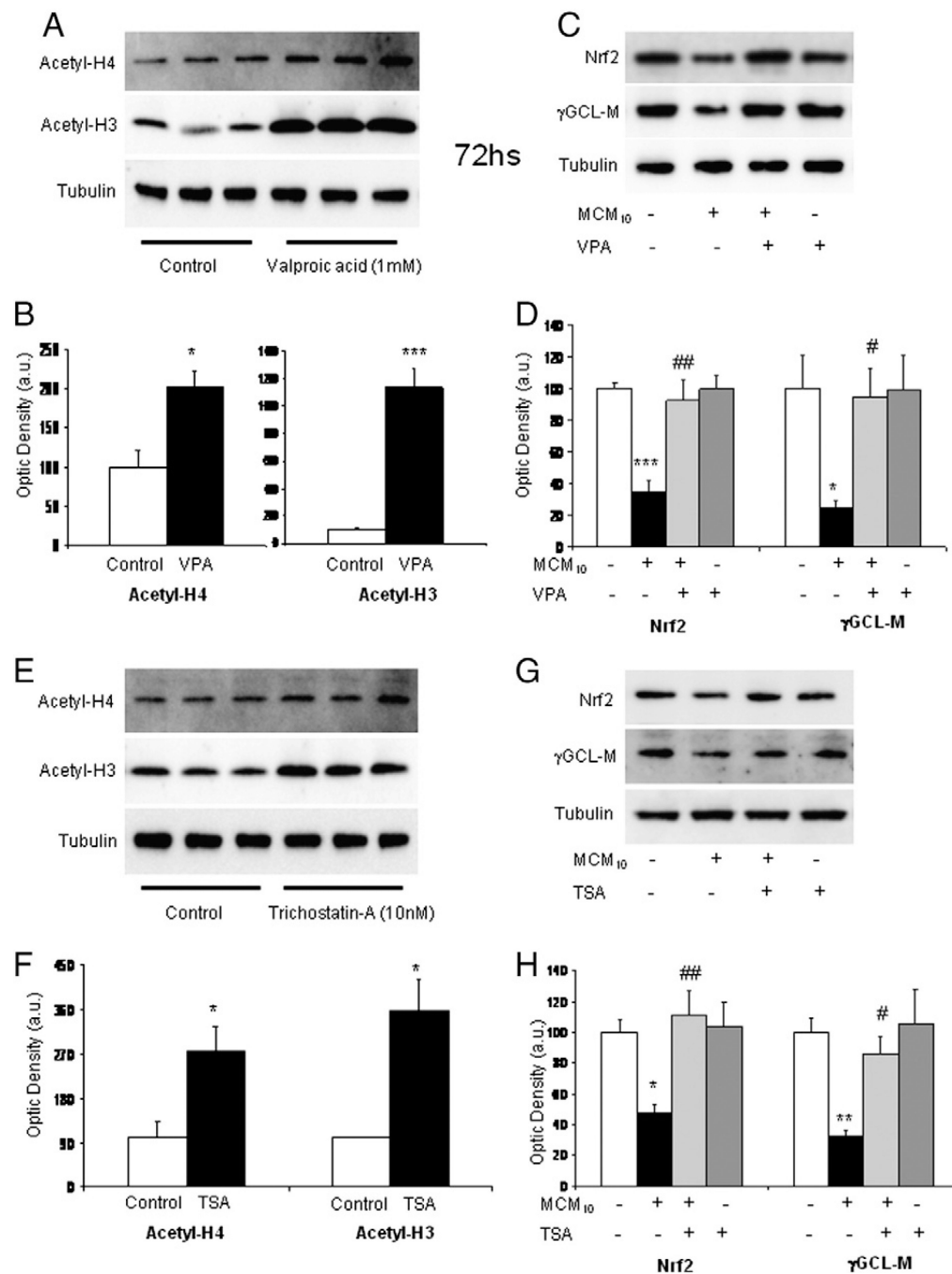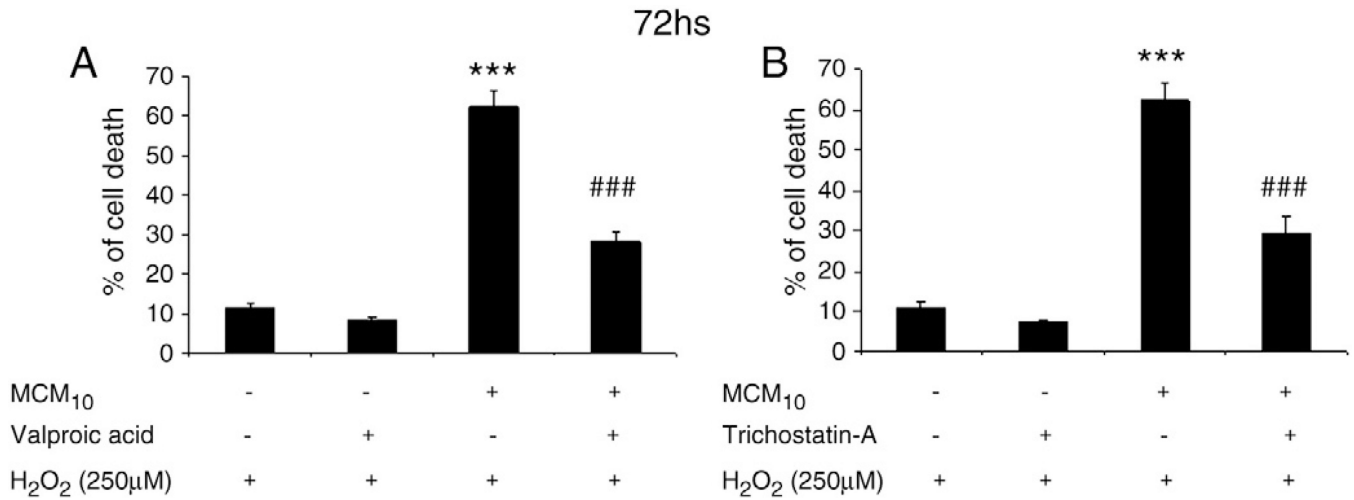
Fig. 6.
(A) Treatment with the HDAC inhibitor valproic acid (VPA; 1 mM) for 72 h induced an increase in the acetylation levels of histones H3 and H4. A representative blot is shown. (B) Densitometric analysis of acetyl-H4 and acetyl-H3 protein expression in astrocyte-rich cultures exposed for 72 h to control conditions or VPA (1 mM). Data are plotted as ratio of the protein of interest/tubulin obtained in each condition. Statistics: *p<0.05 *vs* control; ***p<0.005 *vs* control. (C) Treatment with VPA (1 mM) for 72 h restored the levels of Nrf2 and γGCL-M that were down-regulated by the exposure to MCM_{10}. A representative blot is shown. (D) Densitometric analysis of Nrf2 and γGCL-M protein expression in astrocyte-rich cultures exposed for 72 h to control conditions or MCM_{10} in the presence or absence of

VPA (1 mM). Data are plotted as ratio of the protein of interest/tubulin obtained in each condition. Statistics: *p<0.05 *vs* control; ***p<0.005 *vs* control; #p<0.05 *vs* MCM_{10}; ##p<0.01 *vs* MCM_{10}. (E) Treatment with the HDAC inhibitor trichostatin-A (TSA; 10 nM) for 72 h increased the acetylation levels of histone H3 and histone H4. A representative blot is shown. (F) Densitometric analysis of Acetyl-H4 and Acetyl-H3 protein expression in astrocyte-rich cultures exposed for 72 h to control conditions or TSA (10 nM). Data are plotted as ratio of the protein of interest/tubulin obtained in each condition. Statistics: *p<0.05 *vs* control. (G) Treatment with TSA (10 nM) for 72 h restored the levels of Nrf2 and γGCL-M that were down-regulated by the exposure to MCM_{10}. A representative blot is shown. (H) Densitometric analysis of Nrf2 and γGCL-M protein expression in astrocyte-rich cultures exposed for 72 h to control conditions or MCM_{10} in the presence or absence of TSA (10 nM). Data are plotted as ratio of the protein of interest/tubulin obtained in each condition. Statistics: *p<0.05 *vs* control; **p<0.01 *vs* control; #p<0.05 *vs* MCM_{10}; ##p<0.01 *vs* MCM_{10}.

Fig. 7.
(A) Cells were exposed for 72 h to control conditions or MCM_{10} in the presence or absence of VPA (1 mM). Next, cells were exposed to hydrogen peroxide (250 μM) for 3 h and cell death was assessed by measuring the LDH released into the bathing medium. Long-term exposure to MCM_{10} rendered astrocyte-rich cultures more susceptible to oxidative stress induced by hydrogen peroxide, showing higher levels of cell loss. This effect was partially reversed by the treatment with VPA (1 mM). The results shown are the mean ± SEM. Statistics: ***$p < 0.005$ *vs* control; ###$p < 0.005$ *vs* MCM_{10}. (B) Cells were exposed for 72 h to control conditions or MCM_{10} in the presence or absence of TSA (10 nM). Next, cells were exposed to hydrogen peroxide (250 μM) for 3 h and cell death was assessed by measuring the LDH released into the bathing medium. Prolonged exposure to MCM_{10} rendered astrocyte-rich cultures more susceptible to oxidative stress induced by hydrogen peroxide, showing higher levels of cell loss. This effect was partially reversed by the treatment with TSA (10 nM). The results shown are the mean ± SEM. Statistics: ***$p < 0.005$ *vs* control; ###$p < 0.005$ *vs* MCM_{10}.